

Branching Ratio and Polarization of $B \rightarrow \rho(\omega)\rho(\omega)$ Decays in Perturbative QCD Approach

Ying Li*, Cai-Dian Lü

CCAST (World Laboratory), P.O. Box 8730, Beijing 100080, China;

Institute of High Energy Physics, CAS, P.O.Box 918(4) Beijing 100049, China[†]

December 2, 2024

Abstract

In this work, we calculate the branching ratio, polarization fraction and CP asymmetry of decay modes $B \rightarrow \rho(\omega)\rho(\omega)$ in the Perturbative QCD approach, which is based on \mathbf{k}_T factorization. After calculation, we find the branching ratios of $B^0 \rightarrow \rho^+\rho^-$, $B^+ \rightarrow \rho^+\rho^0$ and $B^+ \rightarrow \rho^+\omega$ are at the order of 10^{-5} , and their longitudinal polarization fractions are more than 90%. The above results agree with BaBar's measurements. We also calculate the branching ratio and polarization fraction of $B^0 \rightarrow \rho^0\rho^0$, $B^0 \rightarrow \rho^0\omega$ and $B^0 \rightarrow \omega\omega$ decays. We find that their longitudinal polarization fractions are suppressed to 60-80% due to a small color suppressed tree contribution. The dominant penguin and non-factorization tree contributions equally contribute to the longitudinal and transverse polarization, which will be tested in the future experiments. We predict the CP asymmetry of $B^0 \rightarrow \rho^+\rho^-$ and $B^+ \rightarrow \rho^+\rho^0$, which will play an important role in determining CKM angle α .

*e-mail: liying@mail.ihep.ac.cn

[†]Mailing address.

1 Introduction

The study of exclusive non-leptonic weak decays of B mesons provides not only good opportunities for testing the Standard Model (SM) but also powerful means for probing different new physics scenarios beyond the SM. The mechanism of two body B decay is still not quite clear, although many physicists devote to this field. The hadronic effects must be important while a reliable calculation of these effects is very difficult [1]. Starting from factorization hypothesis [2], many approaches have been built to explain the existing data and made some progress such as general factorization [3], QCD factorization (BBNS) [4], perturbative QCD Approach (PQCD) [5], and soft-collinear effective theory [6]. These approaches separately explained many of the $B \rightarrow PP$ and $B \rightarrow PV$ decays though many flaws existed in different approaches.

Recently, $B \rightarrow VV$ decays such as $B \rightarrow \phi K^*$ [7], $B \rightarrow \rho K^*$ [8], have aroused many interests of physicists. It is known that both longitudinal and transverse polarization states are possible in $B \rightarrow VV$ decay modes. So, the theoretical analysis of $B \rightarrow VV$ is more complicated than $B \rightarrow PP$ and $B \rightarrow PV$. The predictions of those decays' polarization according to the naive factorization do not agree with the experimental results, although many ideas [9, 10, 11] have been proposed to explain this phenomenon. Some people think that it is a signal of new physics [12, 13].

Very recently, both BaBar and Belle have measured the branching ratios and polarizations of the decays $B^0 \rightarrow \rho^+ \rho^-$ and $B^+ \rightarrow \rho^+ \rho^0$ [14, 15, 16, 17]. The data for the branching ratios and the polarization fractions for these decay channels are reported in Table 1. From this table, we find some decay modes have very large branching ratio. The longitudinal polarization is also very large, which is different with $B \rightarrow \phi K^*$. These results have produced considerable theoretical interest, and many papers [9, 10, 11] focus on these decays. In this paper, we calculate the branching ratios and polarization fractions and predict some CP violation parameters in the perturbative QCD approach.

For simplicity, we work at the rest frame of B meson. For decay $B \rightarrow \rho^+ \rho^-$, the B meson decays to light vector mesons with large momentum. In PQCD's picture, the short distance hard process dominates this decay amplitude, which is the main difference between PQCD

Table 1: Experimental data of CP-averaged branching ratios for $B \rightarrow \rho(\omega)\rho(\omega)$ decays in unit of 10^{-6} and polarization fractions [14, 15, 16].

Mode	BaBar	Belle	CLEO	Average
$B^- \rightarrow \rho^0 \rho^-$	$22.5^{+5.7}_{-5.4} \pm 5.8$	$31.7 \pm 7.1^{+3.8}_{-6.7}$		$26.4^{+6.1}_{-6.4}$
$B^0 \rightarrow \rho^+ \rho^-$	$30 \pm 4 \pm 5$			30 ± 6
$B^0 \rightarrow \rho^0 \rho^0$	< 18		< 1.1	< 1.1
$B^- \rightarrow \rho^- \omega$	$12.6^{+3.7}_{-3.3} \pm 1.8$			$12.6^{+4.1}_{-3.8}$
$B^0 \rightarrow \rho^0 \omega$	< 3.3		< 11	< 3.3
$B^0 \rightarrow \omega \omega$				< 19
$f_L(\rho^0 \rho^-)$	$0.97^{+0.03}_{-0.07} \pm 0.04$	$0.95 \pm 0.11 \pm 0.02$		$0.96^{+0.04}_{-0.07}$
$f_L(\rho^+ \rho^-)$	$0.99 \pm 0.03 \pm 0.04$			0.99 ± 0.05
$f_L(\rho^- \omega)$	$0.88^{+0.12}_{-0.15} \pm 0.03$			$0.88^{+0.12}_{-0.15}$

and BBNS. Because the two light mesons move fast back to back, they have small chance to exchange soft particles, therefore the soft final state interaction may not be important. We argue that a hard gluon emitted from the four quarks operator kicks the spectator quark with big momentum transfer. The formalism of PQCD approach for two-body non-leptonic B meson decays has been given in many papers [5, 18], which is subject to corrections of $\mathcal{O}(\alpha_s)$ and $\mathcal{O}(\bar{\Lambda}/M_B)$. In this factorization theorem, decay amplitude is written as the convolutions of the corresponding hard parts with universal meson distribution amplitudes, which describe hadronic process of the meson. Because the Sudakov effect from k_T and threshold resummation [19], the end point singularities do not appear.

This paper is organized as follows. In Section. 2, we give some explanation about wave functions and convolutions. In Section. 3, we will analyze the processes $B^0 \rightarrow \rho^+ \rho^-$, $B^+ \rightarrow \rho^+ \rho^0$, $B^0 \rightarrow \rho^0 \rho^0$. Some numerical results and CP discussion are given in Section. 4 and 5 respectively. We summarize our work at last.

2 Wave Function & Convolution

2.1 Wave Function

In this paper, we use the light-cone coordinates to describe the four dimension momentum as (p^+, p^-, p^\perp) . In our calculation, the B meson is treated as a heavy-light system. Its wave function is defined as:

$$\begin{aligned}\Phi_{B,\alpha\beta,ij}^{(\text{in})} &\equiv \langle 0 | \bar{b}_{\beta j}(0) d_{\alpha i}(z) | B(p) \rangle \\ &= \frac{i\delta_{ij}}{\sqrt{2N_c}} \int dx d^2\mathbf{k}_T e^{-i(xp^-z^+ - \mathbf{k}_T \mathbf{z}_T)} [(\not{p} + M_B)\gamma_5 \phi_B(x, \mathbf{k}_T)]_{\alpha\beta},\end{aligned}\quad (1)$$

where the indices α and β are spin indices, i and j are color indices, and N_c is the color factor. The distribution amplitude ϕ_B is normalized as

$$\int_0^1 dx_1 \phi_B(x_1, b_1 = 0) = \frac{f_B}{2\sqrt{2N_c}}, \quad (2)$$

where b_1 is the conjugate space coordinate of transverse momentum k_T , and f_B is the decay constant of the B meson. In this study, we use the model function

$$\phi_B(x, b) = N_B x^2 (1-x)^2 \exp \left[-\frac{1}{2} \left(\frac{xM_B}{\omega_B} \right)^2 - \frac{\omega_B^2 b^2}{2} \right], \quad (3)$$

where N_B is the normalization constant and ω_B is the shape parameter. We used $\omega_B = 0.4$ GeV, which is determined by the calculation of form factors and other well known decay modes [5].

As a light-light system, The ρ^- meson wave function of the longitudinal parts is given by [20]

$$\begin{aligned}\Phi_{\rho^-, \alpha\beta, ij} &\equiv \langle \rho(p, \epsilon_L) | \bar{d}_{\beta j}(z) u_{\alpha i}(0) | 0 \rangle \\ &= \frac{\delta_{ij}}{\sqrt{2N_c}} \int_0^1 dx e^{ixp \cdot z} [m_\rho \not{\epsilon}_L \phi_\rho(x) + \not{\epsilon}_L \not{p} \phi_\rho^t(x) + m_\rho \phi_\rho^s(x)]_{\alpha\beta}.\end{aligned}\quad (4)$$

The first term in the above equation is the leading twist wave function (twist-2), while the others are sub-leading twist (twist-3) wave functions. The ρ meson can also be transversely polarized, and its wave function is then

$$\begin{aligned}\langle \rho^-(p, \epsilon_T) | \bar{d}_{\beta j}(z) u_{\alpha i}(0) | 0 \rangle &= \frac{\delta_{ij}}{\sqrt{2N_c}} \int_0^1 dx e^{ixp \cdot z} \left\{ \not{\epsilon}_T [\not{p} \phi_\rho^T(x) + m_\rho \phi_\rho^v(x)] \right. \\ &\quad \left. + \frac{m_\rho}{p \cdot n} i \epsilon_{T\mu\nu\rho\sigma} \gamma_5 \gamma^\mu \epsilon^\nu p^\rho n^\sigma \phi_\rho^a(x) \right\},\end{aligned}\quad (5)$$

where n is moving direction of this particle. Here the leading twist wave function for the transversely polarized ρ meson is the first term which is proportional to ϕ_ρ^T .

The distribution amplitudes of ρ meson, ϕ_ρ , ϕ_ρ^t , ϕ_ρ^s , ϕ_ρ^T , ϕ_ρ^v , and ϕ_ρ^a , are calculated using light-cone QCD sum rule [20]:

$$\phi_\rho(x) = \frac{3f_\rho}{\sqrt{2N_c}}x(1-x) \left[1 + 0.18C_2^{3/2}(2x-1) \right], \quad (6)$$

$$\begin{aligned} \phi_\rho^t(x) = & \frac{f_\rho^T}{2\sqrt{2N_c}} \{ 3(2x-1)^2 + 0.3(2x-1)^2[5(2x-1)^2 - 3] \\ & + 0.21[3 - 30(2x-1)^2 + 35(2x-1)^4] \}, \end{aligned} \quad (7)$$

$$\phi_\rho^s(x) = \frac{3f_\rho^T}{2\sqrt{2N_c}}(1-2x) \left[1 + 0.76(10x^2 - 10x + 1) \right], \quad (8)$$

$$\phi_\rho^T(x) = \frac{3f_\rho^T}{\sqrt{2N_c}}x(1-x) \left[1 + 0.2C_2^{3/2}(2x-1) \right], \quad (9)$$

$$\begin{aligned} \phi_\rho^v(x) = & \frac{f_\rho}{2\sqrt{2N_c}} \left\{ \frac{3}{4}[1 + (2x-1)^2] + 0.24[3(2x-1)^2 - 1] \right. \\ & \left. + 0.12[3 - 30(2x-1)^2 + 35(2x-1)^4] \right\}, \end{aligned} \quad (10)$$

$$\phi_\rho^a(x) = \frac{3f_\rho}{4\sqrt{2N_c}}(1-2x) \left[1 + 0.93(10x^2 - 10x + 1) \right], \quad (11)$$

with the Gegenbauer polynomials,

$$\begin{aligned} C_2^{1/2}(t) &= \frac{1}{2}(3t^2 - 1), \quad C_4^{1/2}(t) = \frac{1}{8}(35t^4 - 30t^2 + 3), \\ C_2^{3/2}(t) &= \frac{3}{2}(5t^2 - 1), \quad C_4^{3/2}(t) = \frac{15}{8}(21t^4 - 14t^2 + 1). \end{aligned} \quad (12)$$

2.2 Convolution

The $B \rightarrow \rho\rho$ decay rates are written as

$$\Gamma = \frac{G_F^2 P_c}{16\pi M_B^2} \sum_{\sigma=L,T} \mathcal{M}^{(\sigma)\dagger} \mathcal{M}^{(\sigma)}, \quad (13)$$

where $P_c \equiv |P_{2z}| = |P_{3z}|$ is the momentum of either of the outgoing vector mesons, and the superscript σ denotes the helicity states of the two vector mesons with $L(T)$ standing for the longitudinal (transverse) component. After analyzing the Lorentz structure, the amplitude $\mathcal{M}^{(\sigma)}$ is decomposed into [21]:

$$\begin{aligned} \mathcal{M}^{(\sigma)} &= \epsilon_{2\mu}^*(\sigma) \epsilon_{3\nu}^*(\sigma) \left[a g^{\mu\nu} + \frac{b}{m_\rho^2} P_1^\mu P_1^\nu + i \frac{c}{m_\rho^2} \epsilon^{\mu\nu\alpha\beta} P_{2\alpha} P_{3\beta} \right], \\ &\equiv M_B^2 \mathcal{M}_L + M_B^2 \mathcal{M}_N \epsilon_2^*(\sigma = T) \cdot \epsilon_3^*(\sigma = T) + i \mathcal{M}_T \epsilon^{\alpha\beta\gamma\rho} \epsilon_{2\alpha}^*(\sigma) \epsilon_{3\beta}^*(\sigma) P_{2\gamma} P_{3\rho}, \end{aligned} \quad (14)$$

with the convention $\epsilon^{0123} = 1$ and the definitions,

$$\begin{aligned}
M_B^2 \mathcal{M}_L &= a \epsilon_2^*(L) \cdot \epsilon_3^*(L) + \frac{b}{m_\rho^2} \epsilon_2^*(L) \cdot P_1 \epsilon_3^*(L) \cdot P_1 , \\
M_B^2 \mathcal{M}_N &= a \epsilon_2^*(T) \cdot \epsilon_3^*(T) , \\
\mathcal{M}_T &= \frac{c}{m_\rho^2} .
\end{aligned} \tag{15}$$

We define the helicity amplitudes,

$$\begin{aligned}
A_0 &= -\xi M_B^2 \mathcal{M}_L , \\
A_{\parallel} &= \xi \sqrt{2} M_B^2 \mathcal{M}_N , \\
A_{\perp} &= \xi m_\rho^2 \sqrt{2(r^2 - 1)} \mathcal{M}_T ,
\end{aligned} \tag{16}$$

with the normalization factor $\xi = \sqrt{G_F^2 P_c / (16\pi M_B^2 \Gamma)}$ and the ratio $r = P_2 \cdot P_3 / m_\rho^2$. These helicity amplitudes satisfy the relation,

$$|A_0|^2 + |A_{\parallel}|^2 + |A_{\perp}|^2 = 1 , \tag{17}$$

following the helicity summation in Eq. (13). We also introduce another equivalent set of helicity amplitudes,

$$\begin{aligned}
H_0 &= M_B^2 \mathcal{M}_L , \\
H_{\pm} &= M_B^2 \mathcal{M}_N \mp m_\rho^2 \sqrt{r^2 - 1} \mathcal{M}_T ,
\end{aligned} \tag{18}$$

with the helicity summation,

$$\sum_{\sigma} \mathcal{M}^{(\sigma)\dagger} \mathcal{M}^{(\sigma)} = |H_0|^2 + |H_+|^2 + |H_-|^2 . \tag{19}$$

Thus, the only work we left is calculating the matrix elements M_L , M_N and M_T .

3 Perturbative calculations

For decay $B \rightarrow \rho\rho$, the related effective Hamiltonian is given by [22]

$$H_{\text{eff}} = \frac{G_F}{\sqrt{2}} \left\{ V_{ud} V_{ub}^* [C_1(\mu) O_1(\mu) + C_2(\mu) O_2(\mu)] - V_{tb}^* V_{td} \sum_{i=3}^{10} C_i(\mu) O_i(\mu) \right\} , \tag{20}$$

where $C_i(\mu)$ ($i = 1, \dots, 10$) are Wilson coefficients at the renormalization scale μ and the four quark operators O_i ($i = 1, \dots, 10$) are

$$\begin{aligned}
O_1 &= (\bar{b}_i u_j)_{V-A} (\bar{u}_j d_i)_{V-A}, & O_2 &= (\bar{b}_i u_i)_{V-A} (\bar{u}_j d_j)_{V-A}, \\
O_3 &= (\bar{b}_i d_i)_{V-A} \sum_q (\bar{q}_j q_j)_{V-A}, & O_4 &= (\bar{b}_i d_j)_{V-A} \sum_q (\bar{q}_j q_i)_{V-A}, \\
O_5 &= (\bar{b}_i d_i)_{V-A} \sum_q (\bar{q}_j q_j)_{V+A}, & O_6 &= (\bar{b}_i d_j)_{V-A} \sum_q (\bar{q}_j q_i)_{V+A}, \\
O_7 &= \frac{3}{2} (\bar{b}_i d_i)_{V-A} \sum_q e_q (\bar{q}_j q_j)_{V+A}, & O_8 &= \frac{3}{2} (\bar{b}_i d_j)_{V-A} \sum_q e_q (\bar{q}_j q_i)_{V+A}, \\
O_9 &= \frac{3}{2} (\bar{b}_i d_i)_{V-A} \sum_q e_q (\bar{q}_j q_j)_{V-A}, & O_{10} &= \frac{3}{2} (\bar{b}_i d_j)_{V-A} \sum_q e_q (\bar{q}_j q_i)_{V-A}.
\end{aligned} \tag{21}$$

Here i and j are $SU(3)$ color indices; the sum over q runs over the quark fields that are active at the scale $\mu = O(m_b)$, i.e., $q \in \{u, d, s, c, b\}$. Operators O_1, O_2 come from tree level interaction, while O_3, O_4, O_5, O_6 are QCD-penguin operators and O_7, O_8, O_9, O_{10} come from electroweak-penguins.

In the PQCD approach, the $B \rightarrow \rho\rho$ decay amplitude is written as the following factorizing formula [18],

$$\begin{aligned}
\mathcal{M} \sim & \int dx_1 dx_2 dx_3 b_1 db_1 b_2 db_2 b_3 db_3 \\
& \times \text{Tr} [C(t) \Phi_B(x_1, b_1) \Phi_\rho(x_2, b_2) \Phi_\rho(x_3, b_3) H(x_i, b_i, t) S_t(x_i) e^{-S(t)}],
\end{aligned} \tag{22}$$

where Tr denotes the trace over Dirac and color indices. $C(t)$ is Wilson coefficient of the four quarks operator which results from the radiative corrections at short distance. Φ_M is wave function which absorbs non-perturbative dynamics of the process, and it is process independent. The hard part H is rather process-dependent and can be calculated in perturbation approach. t is chosen as the largest energy scale in the hard part, to kill the largest logarithm. The jet function $S_t(x_i)$, called threshold resummation, comes from the resummation of the double logarithms $\ln^2 x_i$. $S(t)$ is Sudakov form factor, which is mentioned for many times [5, 18]. Thus, only the hard part is to be calculated.

Similar to the $B \rightarrow \pi\pi$ decay [5], there are eight types of diagrams contributing to $B \rightarrow \rho^+ \rho^-$ decay mode at leading order, which are shown in Fig. 1. They involve two types: the emission and annihilation topologies. Each type is classified into factorizable diagrams, where hard gluon attaches the quark in the same meson, and non-factorizable diagrams, where hard gluon attaches the quark in the different mesons. Through calculating these diagrams, we can get the M_H , where $H = L, N, T$. Because these diagrams are the same as

those of $B \rightarrow \phi K^*$ [7] and $B \rightarrow K^* K^*$ [23], the formulas of $B \rightarrow \rho\rho$ are similar to those of $B \rightarrow \phi K^*$ or $B \rightarrow K^* K^*$. We just need to replace some correspond wave functions, Wilson coefficients and corresponding parameters. So we don't present the detailed formulas in this paper. The reader can find formulas in papers [7] and [23].

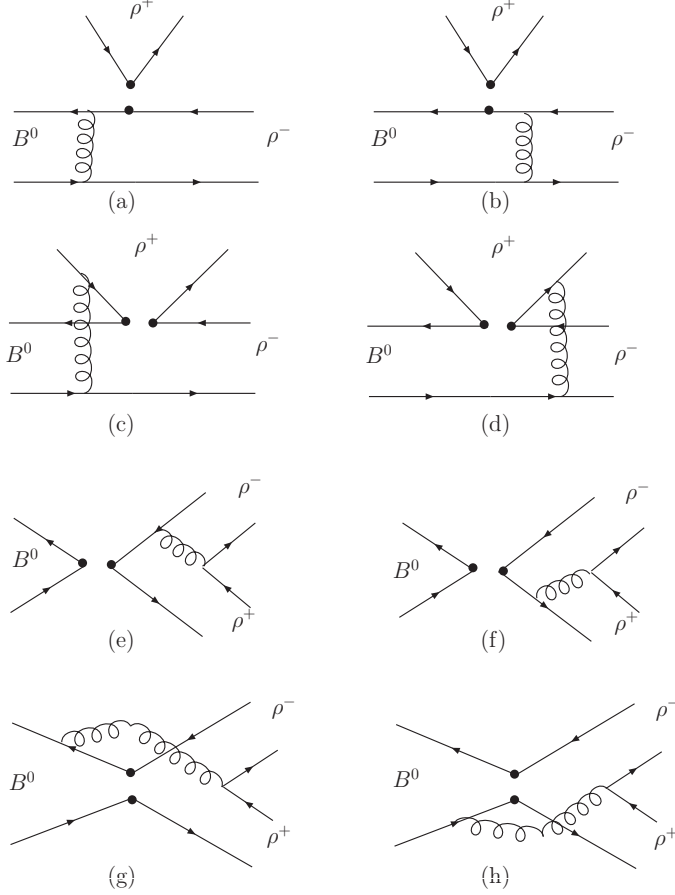


Figure 1: The leading order Feynman diagrams for $B \rightarrow \rho\rho$.

4 Numerical Results and Discussion

In our calculation, some parameters such as meson mass, decay constants, the CKM matrix elements and the lifetime of B meson [24] are given in Table 2. In threshold resummation¹, there is only one parameter c , which is very sensitive to the results, and here we take

¹The formula of threshold resummation [19] is $S_t(x) = \frac{2^{1+2c}\Gamma(3/2+c)}{\sqrt{\pi}\Gamma(1+c)}[x(1-x)]^c$

$c = 0.35$.

Table 2: Parameters we used in numerical calculation [24].

Mass	$m_{B^0} = 5.28\text{GeV}$	$m_{B^+} = 5.28\text{GeV}$
	$m_\rho = 0.77\text{GeV}$	$m_\omega = 0.78\text{GeV}$
Decay	$f_B = 196 \text{ MeV}$	$f_\rho = f_\omega = 200\text{MeV}$
Constants	$f_\rho^\perp = f_\omega^\perp = 160\text{MeV}$	
CKM	$ V_{ud} = 0.9745$	$ V_{ub} = 0.042$
	$ V_{td} = 0.0025$	$ V_{tb} = 0.999$
Lifetime	$\tau_{B^0} = 1.54 \times 10^{-12} \text{ s}$	$\tau_{B^+} = 1.67 \times 10^{-12} \text{ s}$

Taking $\bar{B}^0 \rightarrow \rho^+ \rho^-$ as an example, we know that ($H = L, N, T$):

$$\begin{aligned}
M_H &= V_{ub}V_{ud}^*T_H - V_{tb}V_{td}^*P_H \\
&= V_{ub}V_{ud}^*T_H(1 - \frac{V_{tb}V_{td}^*P_H}{V_{ub}V_{ud}^*T_H}) \\
&= V_{ub}V_{ud}^*T_H(1 + z_H e^{i(\alpha+\delta_H)}),
\end{aligned} \tag{23}$$

with definition: $\alpha = \arg \left[-\frac{V_{tb}V_{td}^*}{V_{ub}V_{ud}^*} \right]$ and $z_H = \left| \frac{V_{tb}V_{td}^*}{V_{ub}V_{ud}^*} \right| \left| \frac{P_H}{T_H} \right|$. In the above functions, angle α is the CKM phase angle, which is a physical parameter. The strong phase δ_H and ratio z_H of tree (T) and penguin (P) are calculated in PQCD approach. In PQCD approach, the strong phases mainly come from the nonfactorizable diagrams and annihilation type diagrams because quarks and gluons can be on mass shell. Numerical analysis also shows that the main contribution to the relative strong phase δ_H comes from the penguin annihilation diagrams. B meson annihilates into $q\bar{q}$ quark pair and then decays to $\rho\rho$ final states [1, 25]. The intermediate $q\bar{q}$ quark pair represents a number of resonance states, which implies final state interaction. In perturbative calculations, the two quark lines can be cut providing the imaginary part. The importance of these diagrams also makes the contribution of penguin diagrams more important than previously expected, since they are chirally enhanced.

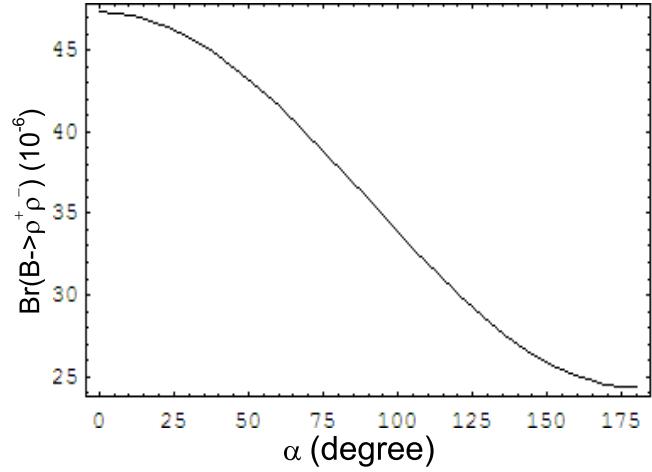


Figure 2: Average branching ratio of $B^0 \rightarrow \rho^+ \rho^-$ with free parameter α .

In the same way , we can get the formula for decay $B^0 \rightarrow \rho^+ \rho^-$:

$$\begin{aligned}
\bar{M}_H &= V_{ub}^* V_{ud} T_H - V_{tb}^* V_{td} P_H \\
&= V_{ub}^* V_{ud} T_H \left(1 - \frac{V_{tb}^* V_{td} P_H}{V_{ub}^* V_{ud} T_H}\right) \\
&= V_{ub}^* V_{ud} T_H (1 + z_H e^{i(-\alpha + \delta_H)}).
\end{aligned} \tag{24}$$

Therefore, the averaged branching ratio for $B \rightarrow \rho^+ \rho^-$ is:

$$\mathcal{M}_H^2 \propto |V_{ub}^* V_{ud} T_H|^2 (1 + 2z_H \cos \alpha \cos \delta_H + z_H^2). \tag{25}$$

Here, we notice the branching ratio is a function of α . If we set α angle as free parameter, we figure out the curve of $B \rightarrow \rho^+ \rho^-$ in Fig. 2, which describes the relation of the branching ratio with angle α . From the figure, we find the branching ratio is about $(25 \sim 47) \times 10^{-6}$. The function of the branching ratio of $B^+ \rightarrow \rho^+ \rho^0$ with angle α is figured out in Fig. 3. It is much less sensitive to the change of CKM angle α , since there is no QCD penguin contribution for this channel.

In Table 3, we show the numerical results of each diagram in $B^0 \rightarrow \rho^+ \rho^-$ decay mode. From this Table, we find that most of the contribution (about 95%) comes from the first two factorizable emission diagrams, especially for the longitudinal part. But the first two diagrams can not contribute to the relative strong phases. From the table, the main source

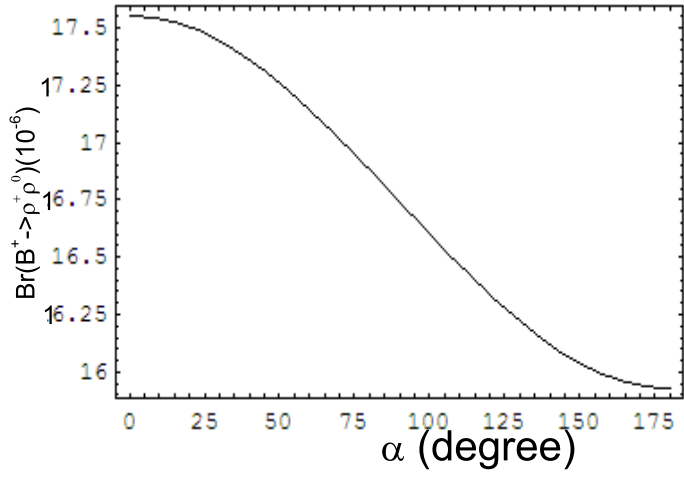


Figure 3: Branching ratio of $B^+ \rightarrow \rho^+ \rho^0$ with free parameter α .

of strong phases are from the annihilation diagrams, especially penguin diagrams of (e) and (f). From this table, we can calculate that $\delta_L = 13.6^\circ$, $\delta_N = 42^\circ$, and $\delta_T = 39^\circ$.

If α change from 60° to 120° , we get the branching ratios:

$$\mathbf{BR}(B^0 \rightarrow \rho^+ \rho^-) = (36 \pm 4) \times 10^{-6}, \quad (26)$$

$$\mathbf{BR}(B^+ \rightarrow \rho^+ \rho^0) = (17 \pm 1) \times 10^{-6}, \quad (27)$$

$$\mathbf{BR}(B^+ \rightarrow \rho^+ \omega) = (19 \pm 1) \times 10^{-6}, \quad (28)$$

$$\mathbf{BR}(B^0 \rightarrow \rho^0 \omega) = (1.9 \pm 0.4) \times 10^{-6}, \quad (29)$$

$$\mathbf{BR}(B^0 \rightarrow \omega \omega) = (1.2 \pm 0.2) \times 10^{-6}, \quad (30)$$

$$\mathbf{BR}(B^0 \rightarrow \rho^0 \rho^0) = (0.9 \pm 0.2) \times 10^{-6}. \quad (31)$$

The branching ratios of decay modes $B^0 \rightarrow \rho^+ \rho^-$, $B^+ \rightarrow \rho^+ \rho^0$ and $B^+ \rightarrow \rho^+ \omega$ are at the order of $\mathcal{O}(10^{-5})$. The decays $B^0 \rightarrow \rho^0 \rho^0$, $B^0 \rightarrow \rho^0 \omega$ and $B^0 \rightarrow \omega \omega$ have much smaller branching ratios due to the fact that they have only color suppressed tree contribution and penguin contribution. We also give the results for polarizations in Table 4 using $\alpha = 90^\circ$. From above results and Table 4, some discussions are in order:

- Comparing our results with experiments in Table 1, we find both branching ratios and polarizations agree with BaBar's data [14, 15] well for decay modes $B^0 \rightarrow \rho^+ \rho^-$,

Table 3: Polarization amplitudes (10^{-3}GeV) of different diagrams in $B^0 \rightarrow \rho^+\rho^-$ decay

Decay mode	(a) and (b)	(c) and (d)	(e) and (f)	(g) and (h)
$L(T)$	77	$-2.4 + 0.6i$	0	$-1.4 - 3.4i$
$L(P)$	-3.1	$0.14 + 0.03i$	$3.0 - 1.7i$	$0.39 + 0.57i$
$N(T)$	8.7	$1.3 - 0.05i$	0	$0.04 - 0.09i$
$N(P)$	-0.34	$-0.03 + 0.007i$	$1.6 + 0.8i$	$-0.002 + 0.009i$
$T(T)$	17	$2.7 - 0.004i$	$0.04 + 0.01i$	$0.002 - 0.008i$
$T(P)$	-1.8	$-0.07 + 0.02i$	$3.2 + 1.7i$	$0.004 + 0.004i$

$B^+ \rightarrow \rho^+\rho^0$ and $B^+ \rightarrow \rho^+\omega$. For Belle, there is only result of $B^+ \rightarrow \rho^+\rho^0$ at present, and their results is larger than ours. We are waiting for the consistent results from two experimental groups. As for the color suppressed $B^0 \rightarrow \rho^0\rho^0$, $B^0 \rightarrow \rho^0\omega$ and $B^0 \rightarrow \omega\omega$, there are only upper limits now, and our results are far below the upper limits.

- In Ref. [12, 26, 27], these decay modes have been calculated in QCD factorization approach. For $B \rightarrow \rho^+\rho^-$, the branching ratio they predicted is a bit larger than the experimental data, because the form factor they used is $V^{B \rightarrow \rho} = 0.338$. In PQCD approach [28], this form factor is about 0.318, so our results is smaller than theirs. Similar to above decay, our results in decay $B^+ \rightarrow \rho^+\rho^0$ is also smaller than results in QCD factorization approach for the same reason. For decay modes $B^0 \rightarrow \rho^0\rho^0$, $B^0 \rightarrow \rho^0\omega$ and $B^0 \rightarrow \omega\omega$, our results are much larger than theirs because the annihilation diagrams play very important role, and these parts cannot be calculated directly in QCD factorization approach.
- From our results, we can see that the branching ratio of $B^0 \rightarrow \rho^+\rho^-$ is about two times of that of $B^+ \rightarrow \rho^+\rho^0$. But in experimental side, the world average results of these decays have not so much difference. Neither QCD factorization approach nor naive factorization can explain this small difference. The same case also appears in the decay $B \rightarrow \pi\pi$ [4, 5]. Many people have tried to explain this puzzle [1, 29]. But for the

$B \rightarrow \rho\rho$ decays, it is still early, since the very small branching ratio of $B^0 \rightarrow \rho^0\rho^0$ by experiments contradicts with isospin symmetry. we have to wait for the experiments.

Table 4: Branching Ratios and Polarizations Fractions of $B \rightarrow \rho(\omega)\rho(\omega)$ Decays

Channel	BR(10^{-6})	$ A_0 ^2(\%)$	$ A_{\parallel} ^2(\%)$	$ A_{\perp} ^2(\%)$
$B^0 \rightarrow \rho^+\rho^-$	35	94	3	3
$B^+ \rightarrow \rho^+\rho^0$	17	94	4	2
$B^+ \rightarrow \rho^+\omega$	19	97	1.5	1.5
$B^0 \rightarrow \rho^0\rho^0$	0.9	60	22	18
$B^0 \rightarrow \rho^0\omega$	1.9	87	6.5	6.5
$B^0 \rightarrow \omega\omega$	1.2	82	9	9

- For the tree dominant decays, most of the contribution to branching ratio comes from factorizable spectator diagram (a) and (b). For decay modes $B^0 \rightarrow \rho^+\rho^-$, the dominant Wilson coefficients are $C_2 + C_1/3$ (order of 1) in tree level, and the results also support the above view. The decay $B^+ \rightarrow \rho^+\omega$ and $B^+ \rightarrow \rho^+\rho^0$ have the similar situation.
- For decay $B \rightarrow \rho^0\rho^0$, the Wilson coefficient is $C_1 + C_2/3$ in tree level, which is color suppressed. In this work, we only calculate the leading order diagrams, and did not calculate the higher order corrections. So, the Wilson coefficients we used are leading order results in order to keep consistency. In leading order, the sign of C_2 is positive while the sign of C_1 is negative, which can cancel each other mostly. Thus the branching ratio of $B \rightarrow \rho^0\rho^0$ is rather small. If considering next leading order corrections, the sign of $C_1 + C_2/3$ may change to positive, so the branching ratio may become larger. This decay should be more sensitive to next leading order contribution. This is similar to the argument of $B^0 \rightarrow \pi^0\pi^0$ decay [30] and $B^0 \rightarrow \rho^0\omega, \omega\omega$.
- For simplicity, we set that the ρ^0 meson, ω have same mass, decay constant and distribution amplitude. In quark model, the ρ^0 meson is $\frac{1}{\sqrt{2}}(u\bar{u} - d\bar{d})$, while ω is

$\frac{1}{\sqrt{2}}(u\bar{u} + d\bar{d})$. The difference comes from the sign of $d\bar{d}$, which only appears in penguin operators, so their difference should be relatively small.

- From the table, we know that longitudinal polarization is dominant in decay $B^0 \rightarrow \rho^+\rho^-$, $B^+ \rightarrow \rho^+\rho^0$ and $B^+ \rightarrow \rho^+\omega$, and occupied more than 90% contribution. This is consistent with the prediction in naive factorization [3], because the transverse parts are r_ρ^2 suppressed, where $r_\rho = m_\rho/m_B$. But for $B^0 \rightarrow \rho^0\rho^0$ decay, the tree emission diagrams are mostly cancelled in the Wilson coefficients. As we will see later in Table 5, the most important contributions for this decay are from the non-factorizable tree diagrams in Fig.1(c,d) and also the penguin diagrams. With an additional gluon, the transverse polarization in the non-factorizable diagrams does not encounter helicity flip suppression. The transverse polarization is at the same order as longitudinal polarization, which can also be seen in the column (c) and (d) of Table 3. This scenario is different from the mechanism of the recently penguin dominant process $B \rightarrow \phi K^*$ [32]. If future experiments do measure the polarization of this channel, it will be a great success of the PQCD approach in the $B \rightarrow VV$ decays. In fact, the $B^0 \rightarrow \omega\omega$ decay has a little larger longitudinal fraction is just due to the fact that there is no non-factorizable emission tree contribution for this decay in isospin symmetry.

Now we turn to discuss the contribution of different diagrams. $B^0 \rightarrow \rho^+\rho^-$ and $B^0 \rightarrow \rho^0\rho^0$ are taken as an example. In the Table 5, we consider full contribution in line (1), ignore annihilation contribution in line (2), without all penguin operator in line (3), and without non-factorization diagram in line (4). From this table, we can see that neither annihilation diagrams nor non-factorizable diagrams can change the polarization fraction in decay $B^0 \rightarrow \rho^+\rho^-$. They only take about 4% contribution in this decay mode just because the emission diagram occupy very large part of the contribution, which also can be seen from Table (3). However, the penguin operators especially in annihilation diagrams play an important role in decay $B^0 \rightarrow \rho^0\rho^0$. The reason has been stated before.

Of course, the final state interaction is very important in non-leptonic B decays. They can give $\mathcal{O}(10^{-6})$ corrections [25], but this can not change the branching ratios much for decay modes $B^0 \rightarrow \rho^+\rho^-$ and $B^+ \rightarrow \rho^+\rho^0$ at order 10^{-5} . Thus, in these two decay modes,

Table 5: Contribution from different parts in $B^0 \rightarrow \rho^+ \rho^-$ and $B^0 \rightarrow \rho^0 \rho^0$: full contribution in line (1), ignore annihilation contribution in line (2), without penguin operators in line (3), and without non-factorization diagrams in line (4)

Class	BR(10^{-6})	$ A_0 ^2(\%)$	$ A_{\parallel} ^2(\%)$	$ A_{\perp} ^2(\%)$
(1)	35	94	3	3
(2)	35	94	3	3
(3)	32	94	3	3
(4)	38	96	2	2
Class	BR(10^{-6})	$ A_0 ^2(\%)$	$ A_{\parallel} ^2(\%)$	$ A_{\perp} ^2(\%)$
(1)	0.94	60	22	18
(2)	0.38	42	26	32
(3)	0.25	18	41	41
(4)	1.18	83	8.5	8.5

the final states interaction may not be important. However, in decay $B^0 \rightarrow \rho^0 \rho^0$, the final states interaction may afford larger contribution than our calculation ($10^{-7} - 10^{-6}$), that's to say, our perturbative part may not be the dominant contribution. The contributions of these two sides can be determined by experiments or other approaches.

There are also many uncertainty factors in our calculation. Firstly, the major uncertainty comes from higher order correction. In calculation of $B \rightarrow K\pi$ [30], the results shows that the next leading order may give about 15% – 20% correction to leading order. Secondly, the wave functions which describe the hadronic process of the meson are not known explicitly, especially for the heavy B meson. ω_B , the only parameter in B meson wave function, can be determined by other channels such as $B \rightarrow \pi l \nu$ [33], $B \rightarrow D\pi$ [34], $B \rightarrow K\pi, \pi\pi$ [5], *etc.* Using the existed data, we can fit the $\omega_B = 0.4$, but this number need more experimental supports. There are still many other uncertain parameters existed such as decay constants, CKM elements, and we will not discuss them here.

5 CP Violation in $B^0 \rightarrow \rho^+ \rho^-$ and $B^+ \rightarrow \rho^+ \rho^0(\omega)$

Searching for CP violation is an important task in B physics. In this section, we will discuss the CP violation in $B^0 \rightarrow \rho^+ \rho^-$ and $B^+ \rightarrow \rho^+ \rho^0$. The uncertainty in $B^0 \rightarrow \rho^0 \rho^0(\omega), \omega\omega$ for branching ratios is so large that we will not discuss their CP violation here, though it is also very important. In decay modes $B^0 \rightarrow \rho^+ \rho^-$ and $B^+ \rightarrow \rho^+ \rho^0$, longitudinal part occupy nearly 95% contribution. So we will neglect the transverse parts in following discussions.

Using Eqs. (23,24), the direct CP violating parameter is

$$\begin{aligned} A_{CP}^{dir} &= \frac{|M^+|^2 - |M^-|^2}{|M^+|^2 + |M^-|^2} \\ &= \frac{-2z \sin \alpha \sin \delta_L}{1 + 2z_L \cos \alpha \cos \delta_L + z_L^2}. \end{aligned} \quad (32)$$

In Fig. 4, We show the direct CP violation parameters as a function of α . The direct CP is about -10% as $\alpha = 110^\circ$ in decay $B^0 \rightarrow \rho^+ \rho^-$. However, the direct CP in decay $B^+ \rightarrow \rho^+ \rho^0$ is almost zero, because there is no QCD penguin contribution and electroweak penguin contribution is rather negligible. On the other hand, because of large penguin contribution, the direct CP in $B^+ \rightarrow \rho^+ \omega$ is about -20% as $\alpha = 110^\circ$, which is even larger than $B^0 \rightarrow \rho^+ \rho^-$.

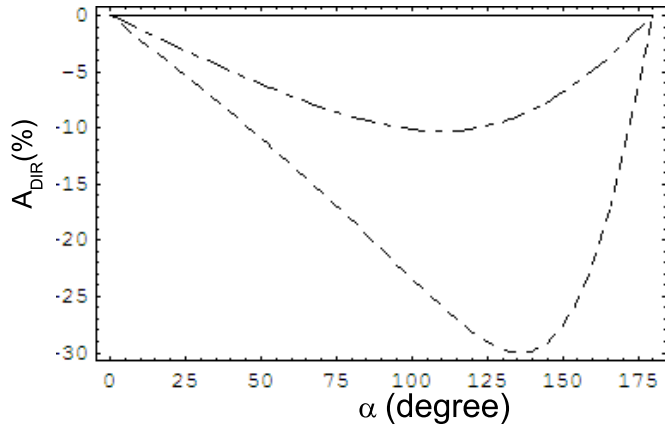


Figure 4: Direct CP violation parameter A_{CP}^{dir} as a function of α . The solid line is for $B^+ \rightarrow \rho^+ \rho^0$, dot-dashed for $B^0 \rightarrow \rho^+ \rho^-$ and dashed line for $B^+ \rightarrow \rho^+ \omega$.

For the neutral B^0 decays, there is more complication from the $B^0 - \bar{B}^0$ mixing. The

time dependence of CP asymmetry is:

$$A_{CP} \simeq A_{CP}^{dir} \cos(\Delta mt) + \sin(\Delta mt) a_{\epsilon+\epsilon'}. \quad (33)$$

In above function, Δm is the mass difference between the two mass eigenstates of neutral B mesons. The A_{CP}^{dir} is already defined in Eq.(32), while the mixing-related CP violation parameter is defined as

$$a_{\epsilon+\epsilon'} = \frac{-2\text{Im}(\lambda_{CP})}{1 + |\lambda_{CP}|^2}, \quad (34)$$

where

$$\lambda_{CP} = \frac{V_{tb}^* V_{td} \langle f | H_{eff} | \bar{B} \rangle}{V_{tb} V_{td}^* \langle f | H_{eff} | B \rangle}. \quad (35)$$

Using Eqs. (23,24), we derive as:

$$\lambda_{CP} \simeq e^{2i\alpha} \frac{1 + z_L e^{i(\delta_L - \alpha)}}{1 + z_L e^{i(\delta_L + \alpha)}}. \quad (36)$$

Thus, the parameter $a_{\epsilon+\epsilon'}$ is a function of α , if the penguin pollution is very small, $a_{\epsilon+\epsilon'}$ is about $-2 \sin 2\alpha$. From the function relation of Fig. 5, we can see that $a_{\epsilon+\epsilon'}$ is not exactly equal to $-2 \sin 2\alpha$, because of the penguin pollution.

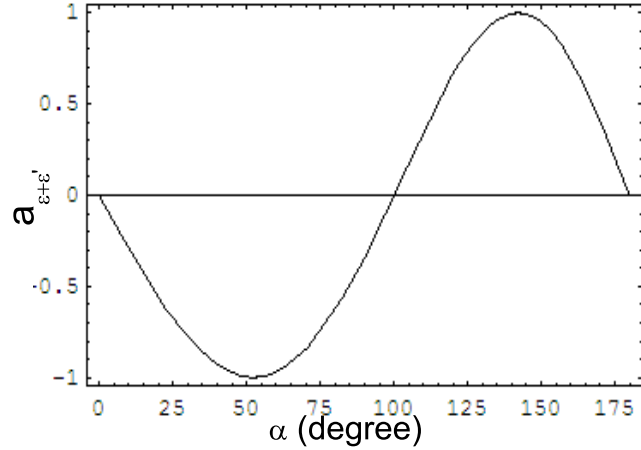


Figure 5: Mixing induced CP violation parameters $a_{\epsilon+\epsilon'}$ of $B^0 \rightarrow \rho^+ \rho^-$, as a function of CKM angle α

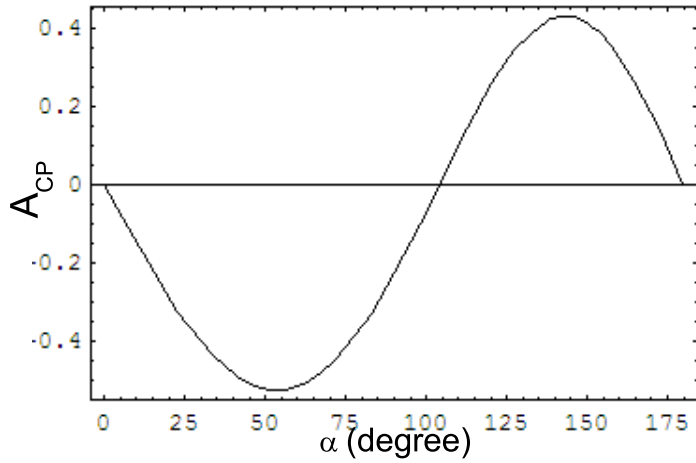


Figure 6: The integrated CP asymmetry of $B^0 \rightarrow \rho^+\rho^-$, as a function of CKM angle α .

If we integrate the time variable t of Eq.(33), we will get the total CP asymmetry as

$$A_{CP} = \frac{1}{1+x^2} A_{CP}^{dir} + \frac{x}{1+x^2} a_{\epsilon+\epsilon'} \quad (37)$$

with $x = \Delta m/\Gamma \simeq 0.771$ for the $B^0 - \bar{B}^0$ mixing in SM [24]. In Fig. (3), we figure out the function as α . In this Figure, we notice that the A_{CP} is 25% when $\alpha = 90^\circ$. If we can measure the CP violation parameter in longitudinal direction, in principal we may determine the angle α .

6 Summary

In this work, we calculate the branching ratios, polarizations and CP asymmetry of $B \rightarrow \rho(\omega)\rho(\omega)$ decay in so-called perturbative QCD approach. After calculating all diagrams, including non-factorizable diagrams and annihilation diagrams, we found the branching ratios of $B^0 \rightarrow \rho^+\rho^-$ and $B^+ \rightarrow \rho^+\rho^0$ are at order of $\mathcal{O}(10^{-5})$, and the longitudinal parts' contribution are more than 95%. These results agree with the BaBar's data well. Moreover, we also predicted the direct CP violation in $B^0 \rightarrow \rho^+\rho^-$ and $B^+ \rightarrow \rho^+\rho^0$, and mixing CP violation in $B^0 \rightarrow \rho^+\rho^-$, all results are important in extraction for the angle α . These parameters can be verified in B factories in future.

Acknowledgments

This work is partly supported by the National Science Foundation of China. We thank C.-H. Chen for useful discussion and G.-L. Song and D.-S. Du for reading the manuscript.

References

- [1] A.J. Buras, R. Fleischer, S. Recksiegel, F. Schwab, Phys. Rev. Lett. 92, 101804 (2004); Nucl. Phys. B697, 133 (2004).
- [2] M. Wirbel, B. Stech, and M. Bauer, Z. Phys. **C29**, 637 (1985); M. Bauer, B. Stech, and M. Wirbel, Z. Phys. **C34**, 103 (1987).
- [3] A. Ali, G. Kramer, C.-D. Lü, Phys. Rev. D58, 094009 (1998), Phys. Rev. D59, 014005 (1999); Y.-H. Chen, H.-Y. Cheng, B. Tseng, K.-C. Yang, Phys. Rev. D60, 094014 (1999).
- [4] M. Beneke, G. Buchalla, M. Neubert, C.T. Sachrajda, Phys. Rev. Lett. 83, 1914 (1999), Nucl. Phys. B591, 313 (2000), Nucl. Phys. B675, 333 (2003).
- [5] H.-N. Li, H.-L. Yu, Phys. Rev. D53, 2480 (1996); Y.-Y. Keum, H.-N. Li, A.I. Sanda, Phys. Rev. D63, 054008 (2001); C.-D. Lu, K. Ukai, M.-Z. Yang, Phys. Rev. D63, 074009 (2001).
- [6] C. W. Bauer, D. Pirjol, I.W. Stewart, Phys. Rev. D65, 054022 (2002); Phys. Rev. D63, 114020 (2001).
- [7] C.-H. Chen, Y.-Y. Keum, H.-N. Li, Phys. Rev. D66, 054013 (2002).
- [8] H.-W. Huang, *et.al*, e-Print Archive: hep-ph/0508080.
- [9] A. L. Kagan, Phys. Lett. B 601, 151 (2004), hep-ph/0407076 .
- [10] P. Colangelo, F. De. Fazio, and T. N. Pham, Phys. Lett. B 597, 291 (2004).
- [11] M. Ladisa, V. Laporta, G. Nardulli, P. Santorelli, Phys. Rev. D70, 114025 (2004).

- [12] Y.-D. Yang, R.-M. Wang, and G.-R. Lu, Phys. Rev. D72, 015009 (2005); S. Bar-shalom, A. Eilam, Y.-D. Yang, Phys. Rev. D 67, 014007 (2003).
- [13] Y. Grossman, Int. J. Mod. Phys. A19, 907 (2004).
- [14] BABAR Collaboration, B. Aubert et al., Phys. Rev. Lett. 91, 171802 (2003).
- [15] BABAR Collaboration, B. Aubert et al., Phys. Rev. D 69, 031102 (2004).
- [16] Belle Collaboration, J. Zhang et al., Phys. Rev. Lett. 91, 221801 (2003).
- [17] BABAR Collaboration, B. Aubert et al., Phys. Rev. Lett. 95, 041805 (2005).
- [18] C.-H Chang, H.-N Li, Phys. Rev. D55, 5577 (1997); T.-W Yeh, H.-N Li, Phys. Rev. D56, 1615 (1997).
- [19] H.-N Li, Phys. Rev. D66, 094010 (2002).
- [20] P. Ball, R. Zwicky, Phys. Rev. D71, 014029 (2005); P. Ball, V.M. Braun, Nucl. Phys. B543, 201 (1999).
- [21] P. Ball, V.M. Braun, Phys. Rev. D58, 094016 (1998).
- [22] G. Buchalla, A. J. Buras, and M. E. Lautenbacher, Rev. Mod. Phys. 68, 1125 (1996).
- [23] J. Zhu, Y.-L. Shen, C.-D. Lü, Phys. Rev. D72, 054015 (2005).
- [24] Particle Data Group, S. Eidelman et al., Phys. Lett. B592, 1 (2004).
- [25] H.-Y. Cheng, Ch.-K. Chua, A. Soni, Phys. Rev. D71 014030 (2005).
- [26] H.-Y. Cheng, K.-C. Yang, Phys. Lett. B511, 40 (2001).
- [27] W.-J Zou, Z.-J Xiao, hep-ph/0507122.
- [28] C.-D. Lü and M.-Z. Yang, Euro. Phys. J. C28, 515 (2003).
- [29] Y.-L. Wu, Y.-F. Zhou, Phys. Rev. D72, 034037 (2005); C.W. Bauer, D. Pirjol, I. Z. Rothstein, I.W. Stewart Phys. Rev. D70, 054015 (2004) and related reference.

- [30] H.-n Li, S. Mishima, A.I. Sanda, hep-ph/0508041.
- [31] K.-F. Chen, et al. (The Belle Collaboration), Phys. Rev. Lett. 94 (2005) 221804; B. Aubert, et al. (The BABAR Collaboration), Phys. Rev. Lett. 93, 231804 (2004).
- [32] H.-N. Li, Phys. Lett. B622, 63-68 (2005); W.-S. Hou, M. Nagashima, hep-ph/0408007.
- [33] H.-N Li, H.-L. Yu, Phys. Rev. Lett. 74, 4388-4391 (1995).
- [34] Y.-Y. Keum, T. Kurimoto, H.-N. Li, C.-D. Lü, A.I. Sanda, Phys. Rev. D69, 094018 (2004).